Long-term physical ageing in As–Se glasses with short chalcogen chains

2008 J. Phys.: Condens. Matter 20 245101

(http://iopscience.iop.org/0953-8984/20/24/245101)

J. Phys.: Condens. Matter **20** (2008) 245101 (7pp) doi:10.1088/0953-8984/20/24/245101

Long-term physical ageing in As–Se glasses with short chalcogen chains

R Golovchak[1,2], O Shpotyuk[1,3], A Kozdras[4], M Vlček[5], B Bureau[6], A Kovalskiy[2] and H Jain[2]

[1] Lviv Scientific Research Institute of Materials of SRC 'Carat', 202, Stryjska street, Lviv, UA-79031, Ukraine
[2] Department of Materials Science and Engineering, Lehigh University, 5, East Packer Avenue, Bethlehem, PA 18015-3195, USA
[3] Institute of Physics of Jan Dlugosz University, 13/15, aleja Armii Krajowej, Czestochowa, 42201, Poland
[4] Faculty of Physics of Opole University of Technology, 75, Ozimska street, Opole, 45370, Poland
[5] Department of General and Inorganic Chemistry, Faculty of Chemistry, University of Pardubice, 532 10 Pardubice, Czech Republic
[6] Verres et Céramiques, UMR CNRS 6226 Sciences Chimiques de Rennes, University of Rennes, 1, Campus de Beaulieu, Rennes, 35042, France

Received 22 January 2008, in final form 7 April 2008
Published 22 May 2008
Online at stacks.iop.org/JPhysCM/20/245101

Abstract
Long-term physical ageing of chalcogenide glasses, which occurs over tens of years, is much less understood than the short-term ageing. With Se-rich underconstrained $As_{30}Se_{70}$ glass as a model composition (consisting of Se_n chains with $n \leqslant 3$ on average), a microscopic model is developed for this phenomenon by combining information from differential scanning calorimetry, extended x-ray absorption fine structure, Raman, and ^{77}Se solid state nuclear magnetic resonance spectroscopies. The accompanying changes in the electronic structure of these glasses are investigated by x-ray photoelectron spectroscopy. The data suggest ageing from cooperative relaxation, presumably involving bond switching or reconfiguration of As–Se–Se–As fragments.

1. Introduction

High transparency in the IR spectral region makes As–Se chalcogenide glasses (ChGs) one of the most promising materials for optoelectronics and IR-fibre optics [1–4]. The fibres drawn for such applications undergo rapid quenching, which introduces a high excess configurational entropy, enthalpy or free volume over the thermodynamic equilibrium state of undercooled liquid [5, 6]. So a thermodynamically driven process known as physical ageing occurs in freshly drawn Se-based optical fibres, tending them to the equilibrium state of undercooled liquid. This is the reason for the structural metastability of ChGs, which can lead to time dependent instability in their mechanical properties [3, 4]. Even thermal annealing near the glass transition temperature T_g does not resolve this problem completely, due to very slow relaxation.

The physical ageing is especially significant in Se-rich ChGs [4, 7, 8], which possess an underconstrained glass network as defined by the Phillips–Thorpe mean-field constraint model [9]. Recently, it was shown that the microstructural nature of physical ageing in such ChGs is strongly connected with Se–Se–Se fragments in their network [8, 10]. The relaxation of inner Se atoms of these atomic fragments within the double-well potential with $\sim kT$ barrier followed by local shrinkage of collapsed Se-rich regions was concluded as the main elementary relaxation act responsible for physical ageing [10]. This process, defined as conventional short-term physical ageing, is characterized by short relaxation times, typically up to a few months or less depending on the composition of the glass. Notably, physical ageing phenomena are also observed in ChGs which do not contain Se–Se–Se segments but are made of underconstrained glass-forming networks (the exact compositional range depends on the coordination of constituent chemical elements) [7]. In such cases, the corresponding relaxation times are ~tens of years; the corresponding effect is appropriately called long-term physical ageing. It is suggested that this process is

associated with general shrinkage of the underconstrained glass matrix, but a proper microstructural mechanism remains to be established [7].

In the present paper, we investigate long-term physical ageing in a Se-based ChG, in which the network approaches a self-organized phase (optimally constrained network) [9] or, equivalently, does not contain Se_n chains or fragments with $n \geqslant 3$, but is still underconstrained. Specifically, the $As_{30}Se_{70}$ composition is selected since its structure is underconstrained and would consist only of As–Se–As and As–Se–Se–As structural fragments according to the 'chain crossing model' [11, 12]. Sometimes, this ChG is considered to be within the so-called 'reversibility window', where no ageing effects should occur [13]. The underlying process is studied by combining the results of differential scanning calorimetry (DSC), x-ray photoelectron spectroscopy (XPS), extended x-ray absorption fine-structure spectroscopy (EXAFS), solid state ^{77}Se nuclear magnetic resonance (NMR) and Raman spectroscopy.

2. Experimental details

Samples of vitreous v-$As_{30}Se_{70}$ were prepared in 1985 by a standard melt-quenching method using a mixture of high purity (99.999%) precursors sealed in evacuated quartz ampoules. Until the present experiment, all ingots were stored in hermetically sealed plastic bags, in the dark at room temperature. The amorphous state of ChG was confirmed visually from the characteristic conch-like fracture and x-ray diffraction data. The glass composition was checked before the experiment by XPS. No significant contamination from the environment (oxygen-based impurities, first of all) was detected in the XPS survey spectra of bulk samples.

A part of the ~20 years aged ChG was rejuvenated before experimental measurements by heating up to a temperature 50 K above T_g and then quenching to room temperature at the same rate. Conditions for this procedure were experimentally established by a set of DSC measurements on As–Se ChGs, aged for different durations, using coincidence of DSC curves after rejuvenation as a criterion. DSC measurements were performed in a DSC 404/3/F microcalorimeter (Netzsch, Germany), which was also used to determine the physical ageing effect in the samples. The heating rate of $q^+ = 5$ K min^{-1} was used for revealing physical ageing by DSC, whereas for rejuvenation $q^- = 5$ K min^{-1} was used in the cooling mode (unless a different cooling rate is mentioned in the text). After this procedure, the samples were in the thermodynamic state close to the initial as-prepared condition due to equilibration of undercooled liquid above T_g [6, 14].

The XPS spectra were recorded with a Scienta ESCA-300 spectrometer using monochromatic Al Kα x-ray (1486.6 eV). All measurements were made on *fresh surfaces of bulk samples broken directly in the ultrahigh vacuum* of an XPS chamber; the angle between the surface and the detector was 90°. The instrument was operated in a mode that yielded a Fermi-level width of 0.4 eV for Ag metal and at a full width at half maximum (FWHM) of 0.54 eV for the Ag $3p_{5/2}$ core-level peak. The XPS data consisted of survey scans over the entire binding energy range and selected scans over the valence band or core-level photoelectron peaks of interest. The surface charging from photoelectron emission was neutralized using a low energy (<10 eV) electron flood gun. Data analysis was conducted with a standard ESCA-300 software package. For analysing the core-level spectra, the Shirley background was subtracted and a Voigt line-shape was assumed for the peaks [15]. Each 3d core-level spectrum for As and Se in our samples consisted of one or more poorly resolved spin orbit doublets ($3d_{5/2}$ and $3d_{3/2}$), whose separation and area ratios were fixed and linked using the data previously obtained for pure element standards. The number of doublets within a given peak was determined by an iterative curve fitting process in which a doublet was added only if it significantly improved the goodness of fit of the experimental data to the envelope of the fitted curve. The uncertainty in the peak position and area of each component was ±0.05 eV and ±2%, respectively.

To perform EXAFS measurements, 20 years aged and rejuvenated samples were powdered and glued onto a 'Kapton' tape. The experiments were performed at the X18B beamline at the National Synchrotron Light Source, Brookhaven National Laboratory. Data were collected at the As K edge (11.863 keV) and Se K edge (12.658 keV) in transmission mode using sealed ion chambers (Oxford Danfysic) filled with Ar/N_2 gases. A standard Athena-Artemis software package [16] was used to process experimental EXAFS spectra to give structural parameters: N_j—number of neighbours in the jth shell at an average distance R_j, and σ_j—the effective Debye–Waller factor representing total disorder. The crystallographic data of the As_2Se_3 crystal [17] were used as input for the fitting.

The Raman spectra were measured with a resolution of 1 cm^{-1} in 100 scans using an IFS 55 Fourier transformation spectrophotometer with FRA 106 accessory (Bruker, Germany). A Nd:YAG laser ($\lambda = 1.064$ μm) with 90 mW output power was used as the excitation beam of the Raman spectra. The raw experimental spectra of aged and rejuvenated samples were processed using Bruker software, normalized by the standard method of matching the most intensive peaks in the studied spectral region and compared by the subtraction method.

The ^{77}Se ($I = 1/2$) NMR measurements were carried out at room temperature on an Avance 300 Bruker spectrometer operating at 57.3 MHz with a 2.5 mm magic angle spinning probe rotating at 22 kHz. Due to the breadth of the NMR lines for glasses, a Hahn spin echo sequence was applied to refocus the whole magnetization. The Fourier transforms were performed on the whole echoes to increase the signal-to-noise ratio and to directly obtain some absorption mode line shapes. Because of slow longitudinal relaxation, the recycle time was equal to 30 s. Due to weak sensitivity, the numbers of scans were chosen between 2000 and 10 000. The experimental spectra were simulated with the Dm2000nt version of the Winfit software [18].

3. Results and discussion

The DSC data for $As_{30}Se_{70}$ ChG after ~20 years of natural storage demonstrate significant natural physical ageing in this

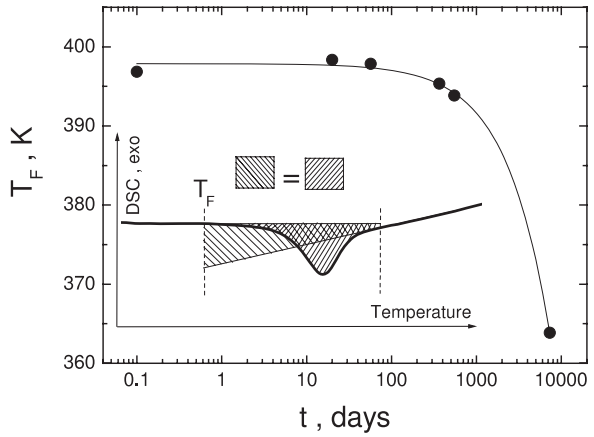

Figure 1. Evolution of fictive temperature T_F during natural storage (the solid line represents the fit; the inset shows the equal square method for T_F calculation [20]).

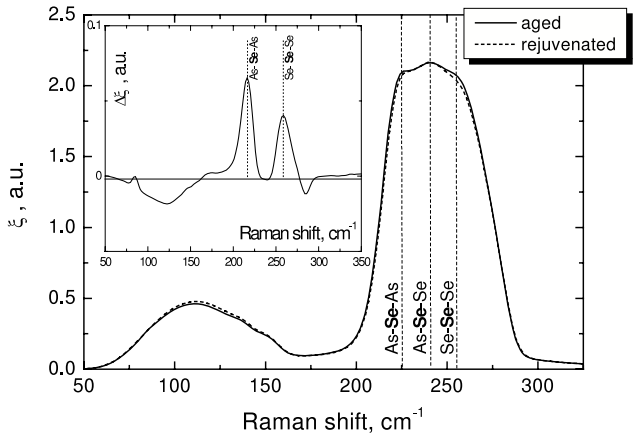

Figure 2. Raman spectra of 20 years aged and rejuvenated vitreous $As_{30}Se_{70}$ samples and their difference (inset).

specimen [7]. It is shown that the observed long-term physical ageing effect is not a consequence of the difference between DSC heating and melt-quenching rates [19]. An additional experiment was performed to investigate the influence of thermal annealing at near-T_g temperatures after synthesis [19]. The results for the $As_{30}Se_{70}$ sample annealed for 24 h at 363 K (∼20 K below T_g) show that physical ageing takes place in this ChG much more effectively at higher temperatures, but it is still much less than the value for the 20 years aged specimen [7, 19]. Thus, even the 24 h annealing of as-prepared samples near T_g does not remove the ageing of this glass completely.

The kinetics of long-term natural physical ageing is investigated for the rejuvenated ($q^- = 5$ K min^{-1}) ChG sample (figure 1). The decrease in fictive temperature (T_F) determined by the equal square method [20] obeys exponential law kinetics, $\exp(-\frac{t}{\tau})$ with characteristic relaxation time $\tau \approx$ 20 years. This magnitude is typical for long-term physical ageing (tens of years) at room temperature, as observed previously in various silicate glasses [21, 22]. So, in principle, the ageing mechanism for underconstrained ChGs without Se–Se–Se fragments associated with network shrinkage may be qualitatively similar to that developed for silicate glasses [23, 24]. However, much lower dissociation energies of chalcogenide bonds (within the ∼1.5–2.8 eV range) [25, 26] compared to that of the Si–O bond (∼4.6 eV) [25], together with the possibility of chalcogen–chalcogen bond formation (in the case of silicate glasses O–O bonds do not exist) [25], introduce an additional possibility for covalent bond switching accompanying physical ageing in ChGs.

To identify likely bond switching during ageing in ChGs we used Raman and solid state ^{77}Se NMR spectroscopy. The obtained results are shown in figures 2 and 3, respectively. The observed peaks in the intensity (ξ) of band components in Raman spectra of aged and rejuvenated ChGs have been assigned to bond-stretching vibrations of directly corner shared (∼230 cm^{-1}) or Se–Se shared (∼240 cm^{-1}) $AsSe_{3/2}$ pyramidal units and Se_3 segments (∼250–260 cm^{-1}) [27–29]. The weak changes after prolonged natural storage are seen in the difference spectrum between aged and rejuvenated samples (see the inset to figure 2). The band of positive intensity change ($\Delta\xi$) at ∼260 cm^{-1} is assigned to the appearance of Se–Se–Se fragments and the one at ∼230 cm^{-1} to the formation of

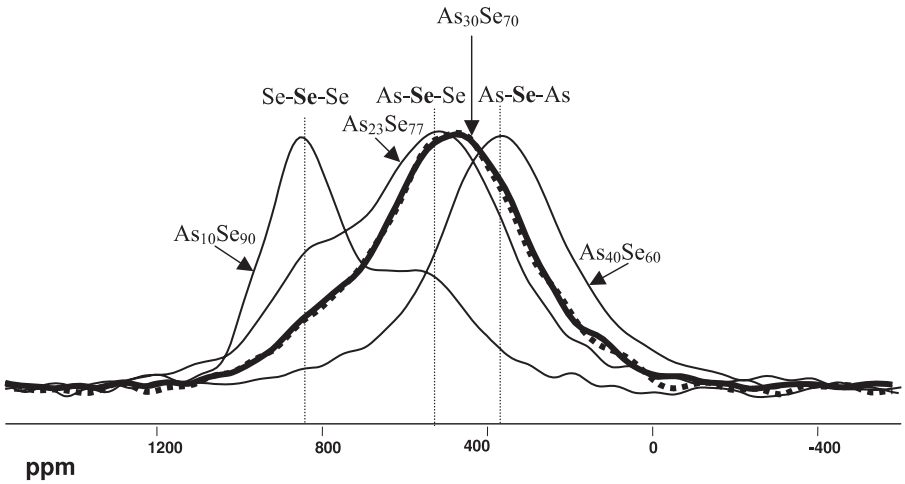

Figure 3. Solid state Se^{77} NMR spectra of 20 years aged (bold solid) and rejuvenated (bold dot) vitreous $As_{30}Se_{70}$ compared to $As_{10}Se_{90}$, $As_{23}Se_{77}$ and $As_{40}Se_{60}$ ChGs taken from [11].

Table 1. Binding energy (BE), full-width at half-maximum (FWHM) of the various structural units obtained from curve fitting of Se $3d_{5/2}$ and As $3d_{5/2}$ core-level spectra. S^0 and S are the fraction of atomic units calculated theoretically using the 'chain crossing model' [11], and from experimental data, respectively.

	Core level															
	As–Se–As				Se–Se–As				Se–Se–Se				Se–As<(Se)$_2$			
Sample	BE (eV)	FWHM (eV)	S (%)	S^0 (%)	BE (eV)	FWHM (eV)	S (%)	S^0 (%)	BE (eV)	FWHM (eV)	S (%)	S^0 (%)	BE (eV)	FWHM (eV)	S (%)	S^0 (%)
Aged	53.97	0.66	32	28	54.38	0.71	62	72	54.82	0.48	6	0	42.27	0.62	100	100
Rejuvenated	53.97	0.69	28	28	54.38	0.82	69	72	54.85	0.45	3	0	42.21	0.72	100	100

As–Se–As fragments or corner shared $AsSe_{3/2}$ pyramids as a result of long-term physical ageing. Then, a decrease in the band intensity due to Se–Se shared $AsSe_{3/2}$ pyramids at ∼240 cm^{-1} is expected, but could not be seen in figure 2 because the presented spectra are matched at this frequency for comparison. We also believe it is masked in the experimental Raman spectra by overlapping with peaks attributed to the former two processes of opposite direction. Analysis of broad features in the 80–150 cm^{-1} range corresponding to bond-bending vibrations is more complicated because of the overlap of different vibrational modes. The slight increase of Se–Se–Se (∼860 ppm) and As–Se–As (∼380 ppm) and decrease of Se–Se–As (∼580 ppm) sites in the structure of aged ChGs can be found by appropriate fitting of ^{77}Se NMR spectra (figure 3) too. The lines are identified from NMR data obtained earlier for vitreous $As_{10}Se_{90}$, $As_{23}Se_{77}$ and $As_{40}Se_{60}$ (figure 3) rich in Se–Se–Se, Se–Se–As and As–Se–As structural fragments, respectively [11, 12]. So, although the observed changes are weak (in the case of NMR they only slightly exceed the noise level), both Raman and NMR methods support the idea that two As–Se–Se–As structural units transform into As–Se–As and As–Se–Se–Se–As fragments during prolonged natural storage.

The same conclusion is supported by high resolution XPS data for Se (figure 4) and As (figure 5) core levels, which allow us to determine the relative fractions of the transformed complexes. Fitting parameters, such as peak position or binding energy (BE), partial area (S) and full width at half maximum (FWHM), are given in table 1. On the basis of electronegativity data [30] and compositional dependence of As–Se XPS spectra [31], the Se 3d doublets (figure 4) with the intensity of primary components at ∼54.8 eV were attributed to Se–Se–Se, at ∼54.4 eV to As–Se–Se and at ∼54.0 eV to As–Se–As structural fragments. The As core level was fitted by only one As 3d doublet with the intensity of the main component at ∼42.2 eV for both aged and rejuvenated samples (figure 5), which was assigned to the Se–As<(Se)$_2$ regular environment. The results in table 1 show that the initial ratio of (Se–Se–Se):(Se–Se–As):(As–Se–As) structural fragments for rejuvenated samples is 3%:69%:28%, which is quite close to the values (S^0 in table 1) theoretically predicted by the 'chain crossing model' for this composition: 0%:72%:28% [11, 12]. After 20 years of natural storage the proportion deviates much more from this model, becoming 6%:62%:32% (table 1). Overall, we can conclude from these XPS results that long-term physical ageing leads to conformation of some Se–Se–As

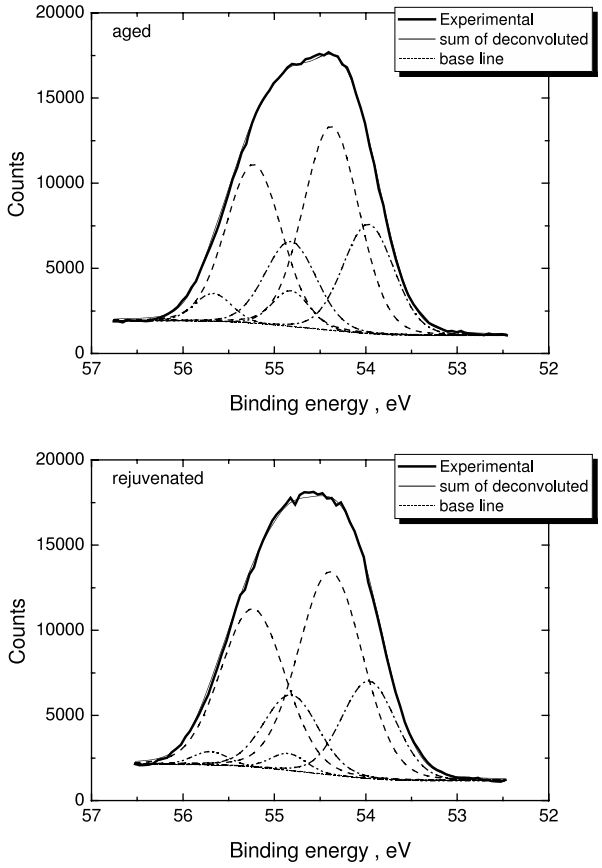

Figure 4. Fitting of Se 3d core-level spectra for $As_{30}Se_{70}$ ChG (dash, dash–dot and dash–dot–dot curves correspond to different fitted components).

complexes into Se–Se–Se and As–Se–As structural fragments, in good agreement with the results obtained by NMR and Raman spectroscopy.

Let us consider four $AsSe_{3/2}$ pyramids coexisting in a manner shown in figure 6. Then, let us assume that I and II pyramidal units are in floppy and III and IV units are in rigid configurations. As an example of such a situation, we can consider III and IV pyramids connected with their environment through direct corner sharing (such a configuration is optimally constrained [9], typical for stoichiometric $As_{40}Se_{60}$ ChG) and I and II pyramids connected with their environment by Se–Se sharing (thus, they are underconstrained). Let us consider a variant when pyramid I in a floppy configuration starts rotating (figure 6) due to some relaxation processes. Since Se–Se (∼1.91 eV) covalent bonds

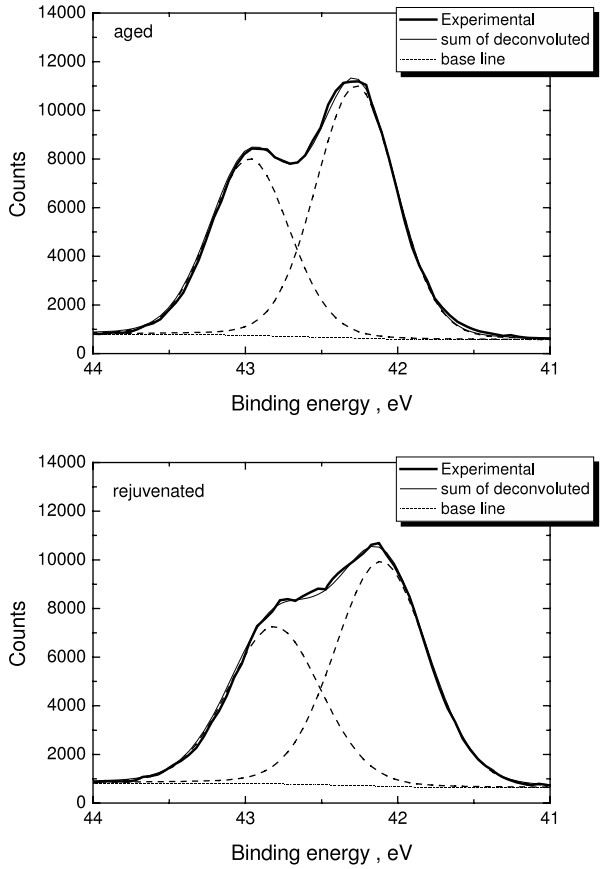

Figure 5. Fitting of As 3d core-level spectra for $As_{30}Se_{70}$ ChG (dash—fitted components).

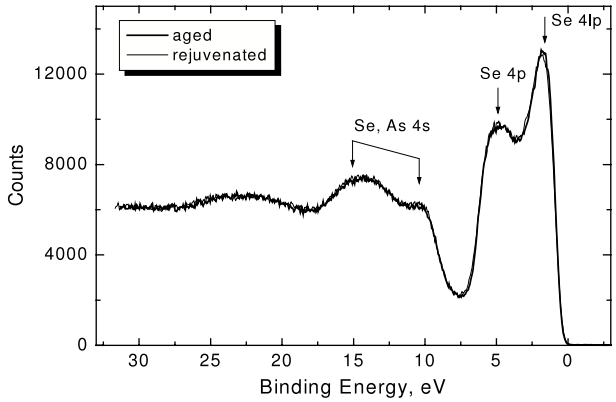

Figure 7. Valence band XPS spectra of aged and rejuvenated $As_{30}Se_{70}$ ChGs.

are stronger than As–Se (∼1.77 eV) bonds [30, 32], the As–Se bond of pyramid II becomes more distorted and finally breaks with greater probability than the Se–Se bond, because the motion of pyramid II is restricted by the environment. The required energy for bond breaking can be accumulated from the appropriate number of atoms or building blocks which participate in the cooperative relaxation process, as in the case of silicate glasses [21, 23].

After the As–Se bond of pyramid II is broken, the switching of the Se–Se bond between pyramids III and IV takes place (figure 6), most probably because of less distortion in the Se–Se bond length/angle within the Se–Se–Se fragment in comparison to those caused by Se–Se sharing of pyramids in rigid configurations. Due to the volume collapse from general shrinkage of the glass matrix (experimentally observed by Chakravarty *et al* [33] and Hatch *et al* [34]), the pyramids II and III become corner shared. We used XPS valence band and EXAFS spectra to ascertain that there is no significant fraction of broken bonds left and that there are no coordination defects (like over-or undercoordinated Se atoms) formed in significant concentrations. The similarity in valence band XPS spectra of aged and rejuvenated samples (figure 7), showing the contribution from 4p lone pair electrons (∼2 eV), 4p bonding states (∼3–5 eV) and 4s electrons (∼11–16 eV) of Se and As [35], is consistent with such a conclusion.

EXAFS is known to be sensitive to the changes in local coordination number around the target atom and to the distances in the coordination shells, as well as to the average deviations in bond lengths and angles (mean square relative displacement or the so-called Debye–Waller factor) [16, 36]. The pronounced peak in partial radial distribution functions associated with the first coordination shell and minor peaks at longer distances attributed to second and further coordination shells were observed for aged and rejuvenated $As_{30}Se_{70}$ ChGs (figure 8), which are typical of glassy materials [36, 37]. For the present work we have analysed only the first coordination shell, which has much better signal-to-noise ratio. The

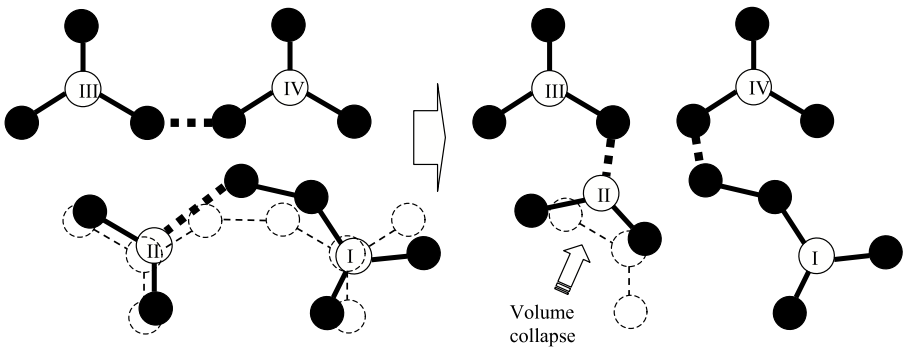

Figure 6. Schematic presentation of bond-changing structural transformations in vitreous $As_{30}Se_{70}$ associated with long-term physical ageing (the switched bonds are highlighted; previous positions of structural complexes are shown by the dashed line).

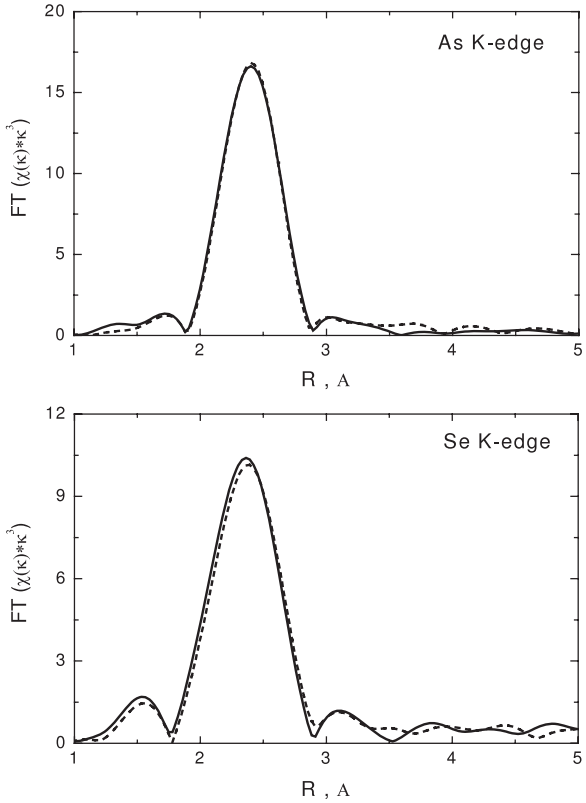

Figure 8. Fourier-transformed k^3-weighted (k is the wavevector of the photoelectron) EXAFS oscillations $\chi(k)$ of $As_{30}Se_{70}$ glass taken at As and Se K-edges in rejuvenated (dash) and 20 year aged (solid) states.

fitting parameters (table 2) do not show any significant changes in average interatomic distances (R_j) or coordination number (N_j) after 20 years of natural storage for both As and Se elements. Thus, we do not find evidence for the formation of coordination defects or broken bonds in significant concentration. More or less noticeable changes are recorded only for Debye–Waller factor (σ^2) from EXAFS spectra of As and Se K edges, which decreases during ageing. Such behaviour can be explained by minimization of bond distortions during ageing through the mechanism described in figure 6. The same conclusion can be drawn from the comparison of FWHM for As and Se core-level XPS spectra (table 1). The decrease in FWHM for the XPS peak of Se–Se–As complexes means disappearance of distorted Se–Se bonds between two pyramidal units in rigid configurations, whereas the decrease in FWHM for As core level can be explained by the ordering of the As environment due to bond rearrangement and volume collapse processes.

4. Conclusions

Long-term physical ageing in underconstrained vitreous $As_{30}Se_{70}$ is attributed to cooperative many-body relaxation dynamics, slowed down by the rigidity of short polymeric Se chains below T_g. The major driving force for physical ageing is volume contraction as in other polymeric materials. It arises from pure shrinkage of the $As_{30}Se_{70}$ underconstrained glass network, as well as the re-conformation of some Se–Se shared $AsSe_{3/2}$ pyramids (As–Se–Se–As structural fragments) into directly corner shared (via As–Se–As bridges) pyramids and Se–Se–Se structural fragments. There is no direct evidence from the present DSC, NMR, XPS, EXAFS and Raman investigations for the formation, in significant concentration, of over- and/or under-coordinated defects either on Se or As atoms, or for the existence of double-bonded Se or broken covalent bonds. The proposed mechanism of physical ageing is expected to be valid for As and/or Ge-based selenide glasses possessing underconstrained glass networks with short Se chains between main structural units (pyramids or tetrahedra).

Table 2. Fitting parameters for Se and As K-edge Fourier-transformed EXAFS spectra of vitreous $As_{30}Se_{70}$: N_j—local coordination number; R—distance from the neighbouring atom to the absorbing atom; σ—standard deviation of the interatomic distance.

Se K edge (12.658 keV)			
Description	N_{Se}	R (Å)	σ^2 (Å^2)
20 years aged	2.0 ± 0.1	2.38 ± 0.01	0.0047 ± 0.0003
Rejuvenated	2.3 ± 0.2	2.39 ± 0.01	0.0060 ± 0.0004
As K edge (11.863 keV)			
Description	N_{As}	R (Å)	σ^2 (Å^2)
20 years aged	3.3 ± 0.3	2.42 ± 0.01	0.0045 ± 0.0004
Rejuvenated	3.6 ± 0.3	2.42 ± 0.01	0.0053 ± 0.0004

Acknowledgments

The authors thank the US National Science Foundation, through the International Materials Institute for New Functionality in Glass (IMI-NFG), for initiating this international collaboration and providing partial financial support (NSF grant No DMR-0409588). Special thanks to Dr S Khalid of Brookhaven National Laboratory, and Drs A Ganjoo and A C Miller of Lehigh University for useful discussions and helpful assistance with the EXAFS and XPS measurements. MV thanks the Czech Ministry of Education, Youth and Sports (project 0021627501) for financial support.

References

[1] Bureau B, Zhang X H, Smektala F, Adam J-L, Troles J, Ma H, Boussard-Pledel C, Lucas J, Lucas P, Coq D L, Riley M R and Simmons J H 2004 *J. Non-Cryst. Solids* **345/346** 276
[2] Churbanov M F, Shiryaev V S, Gerasimenko V V, Pushkin A A, Skripachev I V, Snopatin G E and Plotnichenko V G 2002 *Inorg. Mater.* **38** 1063
[3] McEnroe D J and LaCourse W C 1989 *J. Am. Ceram. Soc.* **72** 1491
[4] Shieh S H M and LaCourse W C 1993 *Mater. Chem. Phys.* **35** 160
[5] Struik L C E 1978 *Physical Ageing in Amorphous Polymers and Other Materials* (New York: Elsevier)
[6] Feltz A 1993 *Amorphous Inorganic Materials and Glasses* (New York: VCH)
[7] Golovchak R, Gorecki Cz, Kozdras A and Shpotyuk O 2006 *Solid State Commun.* **137** 67
[8] Saiter J M, Arnoult M and Grenet J 2005 *Physica* B **355** 370

[9] Thorpe M F, Jacobs D J, Chubynsky M V and Phillips J C 2000 *J. Non-Cryst. Solids* **266–269** 859
[10] Golovchak R, Shpotyuk O, Kozdras A, Bureau B, Vlcek M, Ganjoo A and Jain H 2007 *Phil. Mag.* **87** 4323
[11] Bureau B, Troles J, Le Floch M, Smektala F, Silly G and Lucas J 2003 *Solid State Sci.* **5** 219
[12] Bureau B, Troles J, LeFloch M, Guénot P, Smektala F and Lucas J 2003 *J. Non-Cryst. Solids* **326** 58
[13] Georgiev D G, Boolchand P and Micoulaut M 2000 *Phys. Rev.* B **62** R9228
[14] Pustkova P, Shanelova J, Malek J and Cicmanec P 2005 *J. Therm. Anal. Calorim.* **80** 643
[15] Conny J M and Powell C J 2000 *Surf. Interface Anal.* **29** 856
[16] Ravel B and Newville M 2005 *J. Synchrotron Radiat.* **12** 537
[17] Renninger A L and Averbach B L 1973 *Acta Crystallogr.* B **29** 1583
[18] Massiot D, Fayon F, Capron F, King I, Calvé S Le, Alonso B, Durand J O, Bujoli B, Gan Z and Hoatson G 2002 *Magn. Reson. Chem.* **40** 70
[19] Golovchak R, Kozdras A and Shpotyuk O 2007 *Phys. Lett.* A **370** 504
[20] Moynihan C T, Easteal A J and Wilder J 1974 *J. Phys. Chem.* **78** 2673
[21] Nemilov S V 2000 *Glass Phys. Chem.* **26** 511
[22] Nemilov S V 2001 *Glass Phys. Chem.* **27** 214
[23] Nemilov S V and Johari G P 2003 *Phil. Mag.* **83** 3117
[24] Ngai K L 2005 *J. Non-Cryst. Solids* **351** 2635
[25] Varshneya A K 2006 *Fundamentals of Inorganic Glasses* (Sheffield: Society of Glass Technology)
[26] Pauling L 1967 *The Nature of the Chemical Bond* 3rd edn (New Delhi: Oxford and IBH)
[27] Kovanda V, Vlcek M and Jain H 2003 *J. Non-Cryst. Solids* **326/327** 88
[28] Bogomolov M, Poborchy V V, Romanov S G and Shagin S I 1985 *J. Phys. C: Solid State Phys.* **18** L313
[29] Yannopoulos S N and Andrikopoulos K S 2004 *J. Chem. Phys.* **121** 4747
[30] Pauling L 1960 *The Nature of the Chemical Bond* (Ithaca, NY: Cornell University Press)
[31] Golovchak R, Kovalskiy A, Miller A C, Jain H and Shpotyuk O 2007 *Phys. Rev.* B **76** 125208
[32] Tichy L and Ticha H 1995 *J. Non-Cryst. Solids* **189** 141
[33] Chakravarty S, Georgiev D G, Boolchand P and Micoulaut M 2005 *J. Phys.: Condens. Matter* **17** L1
[34] Hatch C T, Cerqua-Richardson K, Varner J R and LaCourse W C 1997 *J. Non-Cryst. Solids* **209** 159
[35] Jain H, Krishnaswami S, Miller A C, Krecmer P, Elliott S R and Vlcek M 2000 *J. Non-Cryst. Solids* **274** 115
[36] Chen G, Jain H, Khalid S, Li J, Drabold D A and Elliott S R 2001 *Solid State Commun.* **120** 149
[37] Kolobov A V, Oyanagi H, Tanaka K and Tanaka Ke 1996 *J. Non-Cryst. Solids* **198–200** 709